Supplemental Materials for

Tumor-targeted interleukin-12 synergizes with entinostat to overcome PD-1/PD-L1 blockade-resistant tumors harboring MHC-I and APM deficiencies

by Minnar et al.

SUPPLEMENTAL FIGURES 1-7
SUPPLEMENTAL TABLES 1-2
SUPPLEMENTAL METHODS

Minnar CM, *et al. J Immunother Cancer* 2022; 10:e004561. doi: 10.1136/jitc-2022-004561

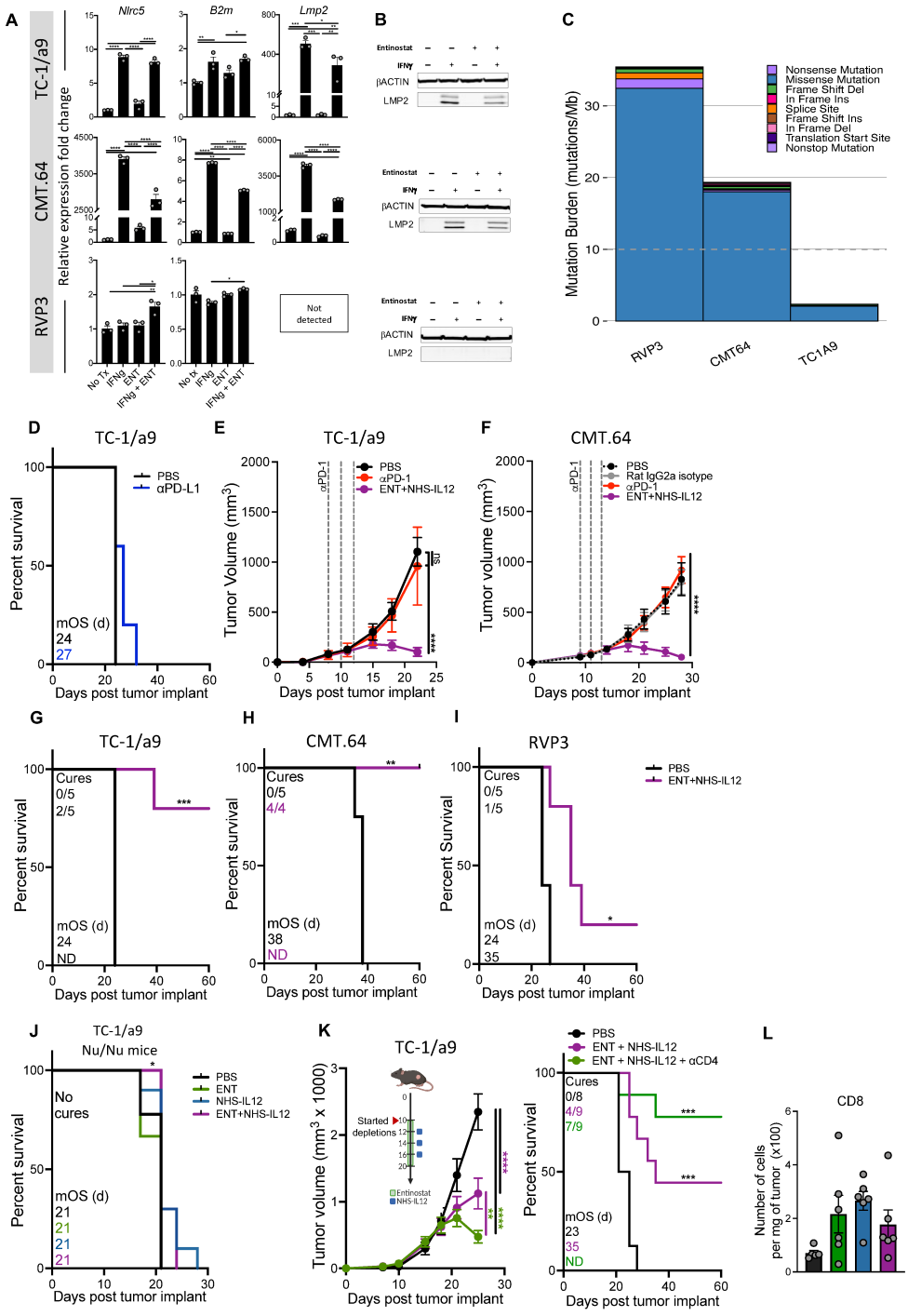
A
TC-1/a9
CMT.64
RVP3
Relative expression fold change
Nlrc5
B2m
Lmp2
No Tx
IFNg
ENT
IFNg + ENT
Not detected
B
Entinostat
IFNγ
βACTIN
LMP2
C
Mutation Burden (mutations/Mb)
Nonsense Mutation
Missense Mutation
Frame Shift Del
In Frame Ins
Splice Site
Frame Shift Ins
In Frame Del
Translation Start Site
Nonstop Mutation
RVP3
CMT64
TC1A9
D
TC-1/a9
PBS
αPD-L1
Percent survival
mOS (d)
24
27
Days post tumor implant
E
TC-1/a9
αPD-1
PBS
αPD-1
ENT+NHS-IL12
Tumor Volume (mm3)
ns
****
Days post tumor implant
F
CMT.64
αPD-1
PBS
Rat IgG2a isotype
αPD-1
ENT+NHS-IL12
Tumor volume (mm3)
****
Days post tumor implant
G
TC-1/a9
Cures
0/5
2/5
***
mOS (d)
24
ND
Percent survival
Days post tumor implant
H
CMT.64
Cures
0/5
4/4
**
mOS (d)
38
ND
Percent survival
Days post tumor implant
I
RVP3
PBS
ENT+NHS-IL12
Cures
0/5
1/5
*
mOS (d)
24
35
Percent Survival
Days post tumor implant
J
TC-1/a9
Nu/Nu mice
PBS
ENT
NHS-IL12
ENT+NHS-IL12
No cures
mOS (d)
21
21
21
21
Percent survival
Days post tumor implant
K
TC-1/a9
Started depletions
Entinostat
NHS-IL12
Tumor volume (mm3 x 1000)
****
**
****
Days post tumor implant
PBS
ENT + NHS-IL12
ENT + NHS-IL12 + αCD4
Cures
0/8
4/9
7/9
***
***
mOS (d)
23
35
ND
Percent survival
Days post tumor implant
L
CD8
Number of cells per mg of tumor (x100)

Supplemental Figure 1. Entinostat and NHS-IL12 combination shows potent anti-tumor efficacy in anti-PD-L1-resistant tumor models harboring APM deficiencies. (A-B) TC-1, TC-1/a9, CMT.64 and RVP3 cell lines were left untreated or treated with entinostat (0.5μM) for 72 hours and/or with IFNγ (0.1μg/ml) for 24 hours and subsequently analyzed by RT-qPCR or western blot. **(A)** Relative fold gene expression ($2^{-\Delta\Delta Ct}$) for APM genes *Nlrc5, B2m* and *Lmp2 (Psmb9*) in TC-1/a9, CMT.64 and RVP3 cell lines. **(B)** Western blot for LMP2 (*Psmb9*) protein expression in TC-1/a9, CMT.64 and RVP3 cell lines. Whole exome sequencing was completed for TC-1/a9, CMT.64 and RVP3 cell lines. **(C)** Tumor mutational burden for each cell line including type of mutation. **(D)** Graph show survival for TC-1/a9-tumor bearing mice treated with PBS (100μl, i.p.) or αPDL1 (200μg, i.p.) as described in Fig. 1C, n=4-5 mice/group. (**E-F**) Graph shows (**E**) TC-1/a9 and (**F**) CMT.64 tumor growth curves in mice treated with aPD-1 isotype control (rat IgG2a) and/or PBS (100μl, i.p.), αPD-1 (200μg, i.p.), or entinostat (6mg/kg/day, p.o.) + NHS-IL12 (2 μg, s.c.) as described in the respective insect schematics, n=3-4 mice/group. **(G-I)** Survival plots of **(G)** TC-1/a9, **(H)** CMT.64, and **(I)** RVP3 tumor-bearing C57Bl/6 mice treated with PBS or entinostat (6mg/kg/day, p.o.) + NHS-IL12 (2 μg, s.c.) as described in Fig. 1F-1H, respectively, n=4-5 mice/group. **(J)** Survival of TC-1/a9 tumor-bearing nu/nu mice as described in Fig. 1K, n=9-10 mice/group. **(K)** Treatment schedule, tumor growth curves, and survival for TC-1/a9 tumor-bearing mice treated with PBS, or combination therapy with and without CD4 T depletion, n=4-9 mice/group. Insets denote number of cured mice per treatment group, and median overall survival (mOS) in days; ND=not determined. **(L)** TC-1/a9 tumor-bearing mice treated with PBS, entinostat (6mg/kg/day, p.o.), NHS-IL12 (2 μg, s.c.) or entinostat + NHS-IL12 were sacrificed 7 days post last dose of NHS-IL12 as described in Fig. 1I, n=5-6 mice/group. Graph shows $CD8^+$ TILs as numbers per mg of tumor. All graphs show mean

± SEM; data are representative 2-3 independent studies (A-B) or 1 independent study (C). For in vivo studies, data are representative of 1-2 independent experiments with n=4-5 mice/group (D-I, L) or 9-10 mice/group (J-K). Survival: Mantel-cox; Bar graphs: one-way ANOVA with Tukey's multiple comparisons test; *= $P < 0.05$, **= $P < 0.01$, ***= $P < 0.001$, ****= $P < 0.0001$.

TIL, tumor-infiltrating lymphocyte.

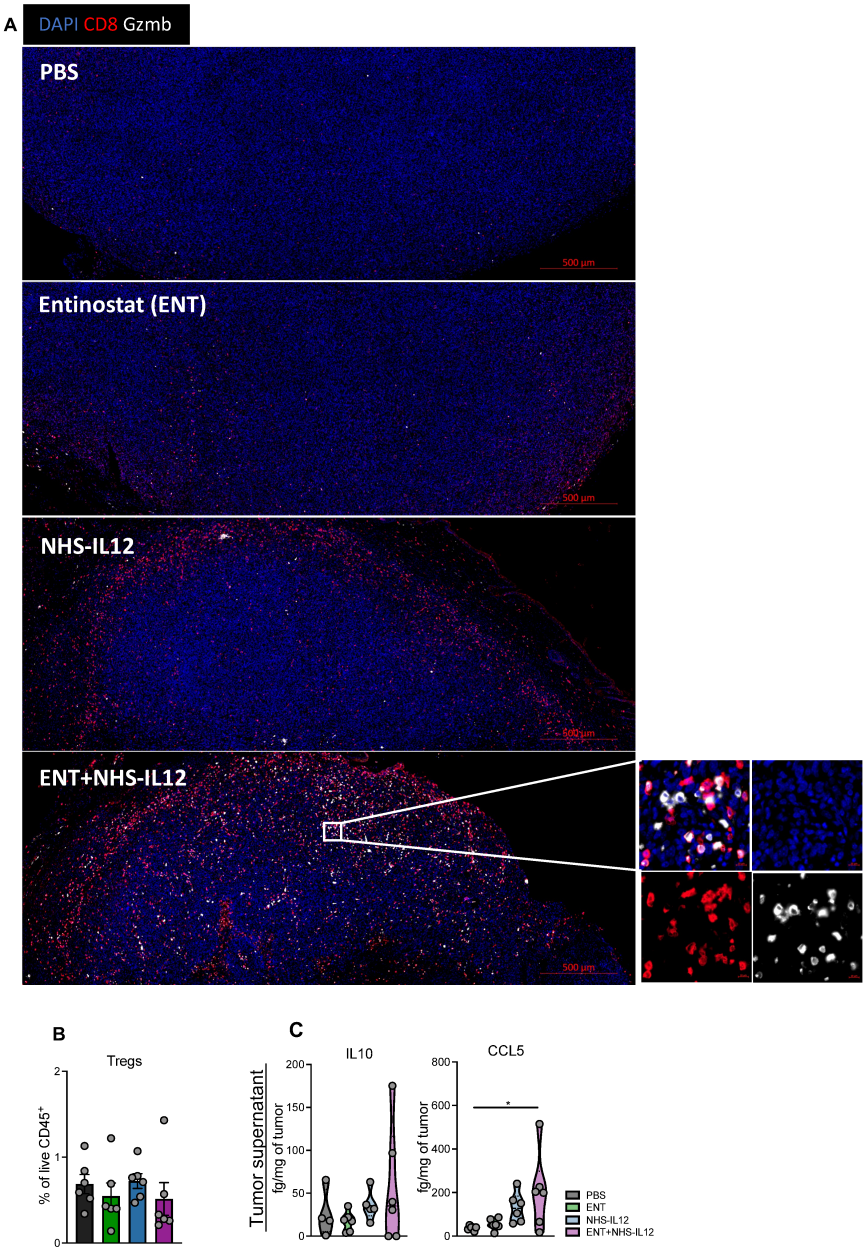

Supplemental Figure 2. Spatial analysis of TC-1/a9 tumors reveals increased CD8 TILs and granzyme B expression in entinostat and NHS-IL12 combination-treated mice. (A) Representative images of immune fluorescent staining for DAPI (blue), CD8 (red) and granzyme B (white); scale bar, 500 µm. **(B-C)** TC-1/a9 tumor-bearing mice treated with PBS, entinostat

(6mg/kg/day, p.o.), NHS-IL12 (2μg, s.c.) or entinostat + NHS-IL12 were sacrificed 7 days post last dose of NHS-IL12 as described in Fig. 1I, n=5-6 mice/group. **(B)** Tumor Tregs as frequency of $CD45^+$ cells. **(C)** Levels of IL-10 and CCL5 in the TME. All graphs show mean ± SEM; data is representative of 1-2 independent experiments. Bar graphs: one-way ANOVA with Tukey's multiple comparisons test; *=P<0.05, **=P<0.01, ***=P<0.001, ****=P<0.0001.

TIL, tumor-infiltrating lymphocyte; TME, tumor microenvironment; Tregs, regulatory T cells.

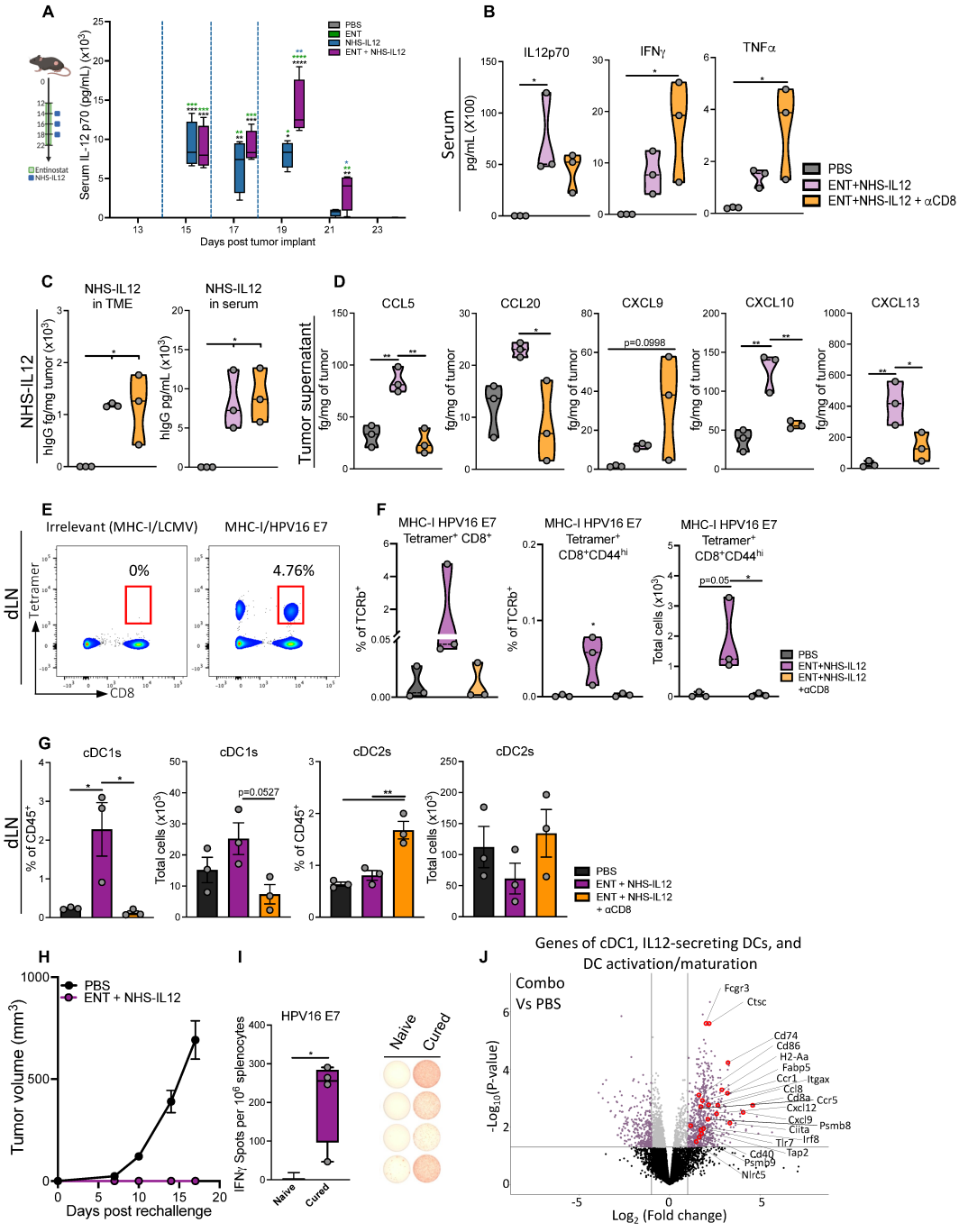

Supplemental Figure 3. Combination therapy mediates chemokine signaling pathways and antigen specific memory. (A) Serum IL12p70 kinetics in TC-1/a9 tumor-bearing mice as

treated in schematic (blue dashed line indicates timing of NHS-IL12 dosing), n=4 mice/group. **(B-I)** TC-1/a9 tumor-bearing mice treated as in Fig. 1L were sacrificed on day 18 (2 days post last dose of NHS-IL12) for cytokines, chemokines, and flow cytometric analyses in the TME and serum, n=3 mice/group. **(B)** Levels of designated cytokines in the serum. **(C)** Levels of NHS-IL12 in tumor and serum. **(D)** Levels of designated chemokines in the TME. **(E)** Representative dot plot showing MHC-I/HPV16 E7 tetramer^{+}CD8^{+} T cells in draining lymph nodes (dLN). **(F)** Frequency of TCRβ^{+} and absolute numbers of cells that are tetramer^{+} CD8^{+} T cells and tetramer^{+} CD8^{+}CD44^{hi} T cells in dLNs. **(G)** cDC1 and cDC2 cells as frequency of CD45^{+} cells and absolute numbers in dLNs. **(H)** TC-1/a9 tumor re-challenge growth curves of mice cured by combination treatment as in Fig. 1L, and naïve mice. **(I)** Quantification of IFNγ by ELIspot in splenocytes from TC-1/a9 rechallenged naïve and cured mice activated by HPV16 E7 15-mer peptide with representative images. (**J**) TC-1/a9 tumor-bearing mice treated as in Fig. 1I were sacrificed on day 25 post-tumor implant and tumor whole transcriptome analysis was performed, n=3-4 mice/group. Volcano plots show differentially expressed genes ($p<0.05$) related to cross-presenting cDC1 or IL12-secreting dendritic cells for combination therapy relative to PBS control; right upper quadrant shows genes upregulated. Horizontal lines indicate threshold for significant changes in gene expression. For schemas, green area represents time course of entinostat treatment (6mg/kg/day, p.o.) and blue squares denote NHS-IL12 dosing (2 μg, s.c.). Graphs show mean ± SEM from 2 independent experiments, (A-I) n=3-4 mice/group. Tumor volumes: two-way ANOVA; Box plots: Two-way ANOVA with Tukey's multiple comparisons test; Bar graphs and violin plots: One-way ANOVA with Tukey's multiple comparisons test or two-tailed unpaired t test (I); *=$P < 0.05$, **= $P < 0.01$, ***= $P < 0.001$, ****= $P < 0.0001$. cDC1, conventional type 1 dendritic cell; TME, tumor microenvironment.

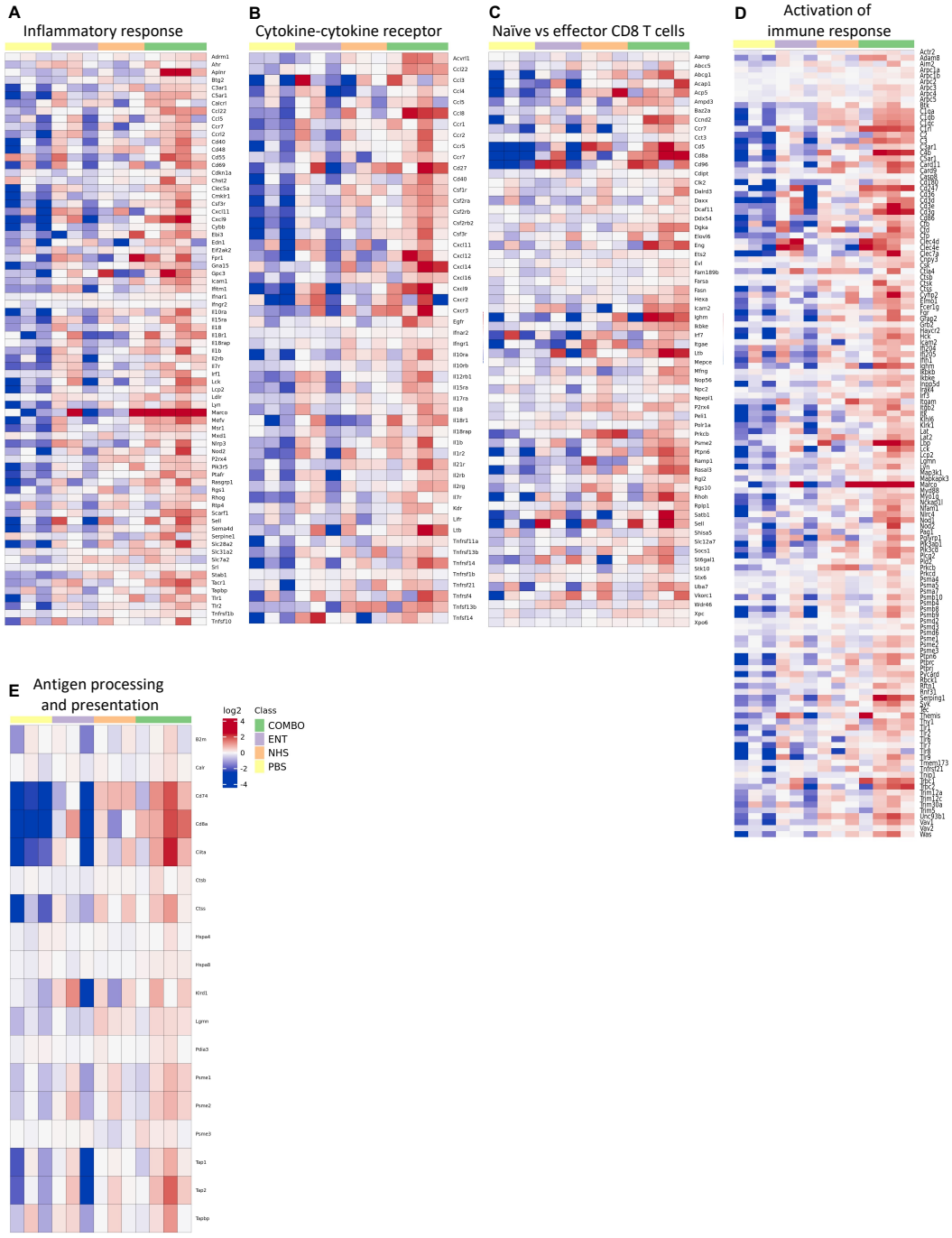
A
Inflammatory response
B
Cytokine-cytokine receptor
C
Naïve vs effector CD8 T cells
D
Activation of immune response
E
Antigen processing and presentation
log2
4
2
0
-2
-4
Class
COMBO
ENT
NHS
PBS

Supplemental Figure 4. Transcriptomic analysis of TC-1/a9 tumors shows enrichment of pathways clinically described as hallmarks of checkpoint blockade resistance. TC-1/a9 tumor-bearing mice treated as in Fig. 1I were sacrificed on day 25 post-tumor implant and tumor whole transcriptome analysis was performed. Gene set enrichment analysis was carried out for entinostat + NHS-IL12 combination-treated tumors compared to PBS. Heatmaps corresponding to enrichment plots (Fig. 4C-H) show significantly altered genes for **(A)** Hallmark inflammatory response, **(B)** KEGG cytokine-cytokine receptor interaction, **(C)** GOLDRATH naïve vs effector CD8 T cell response, **(D)** GO activation of immune response, and **(E)** KEGG antigen processing and presentation pathways. Graphs represent 1 experiment, n=3-4 mice/group.

GO, gene ontology.

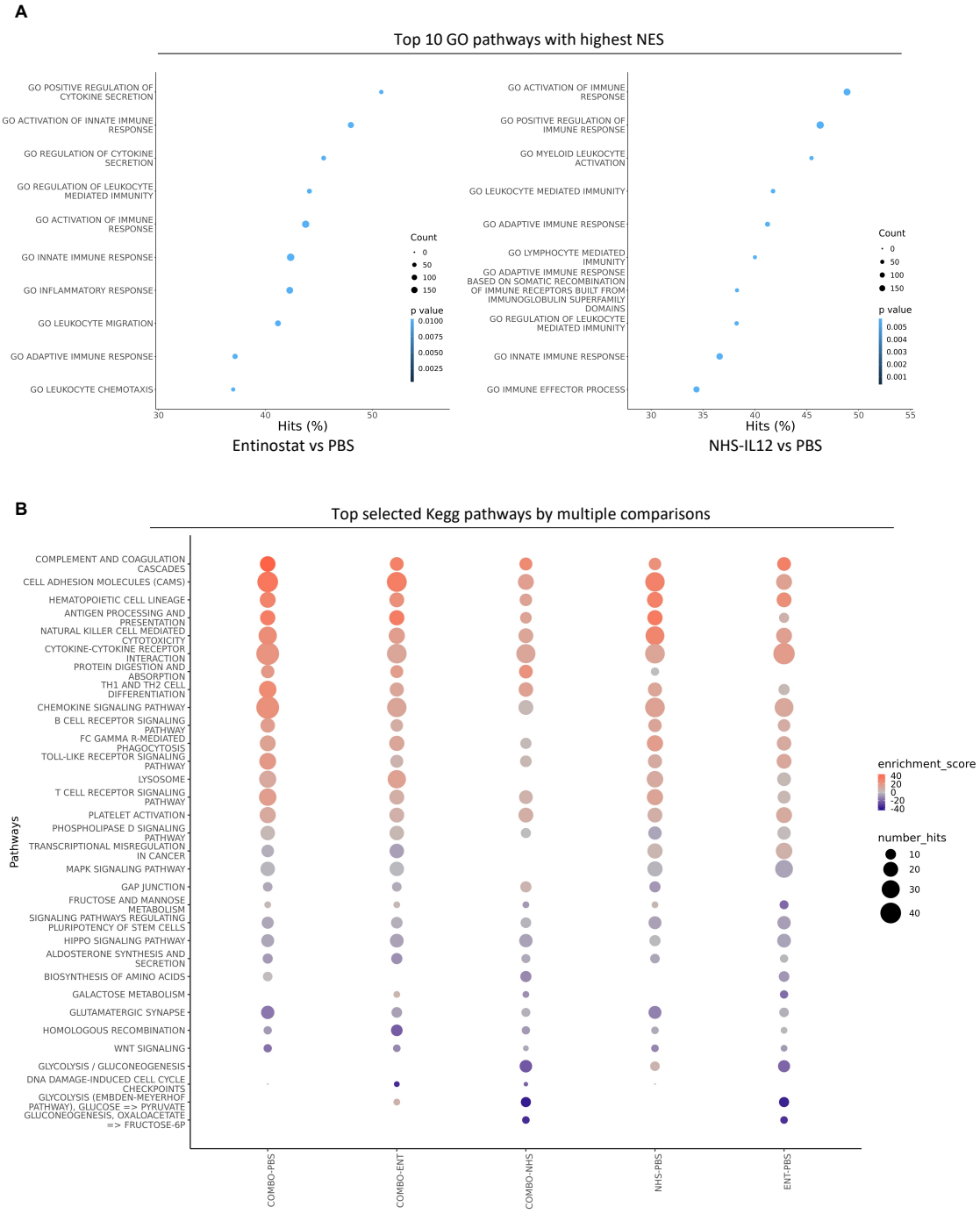

Supplemental Figure 5. Transcriptomic analysis of TC-1/a9 tumors showing combination versus single treatments. TC-1/a9 tumor-bearing mice treated as in Fig. 1I were sacrificed on

day 25 post-tumor implant and tumor whole transcriptome analysis was performed. Gene set enrichment analysis was carried out for entinostat alone and NHS-IL12 alone versus PBS-treated tumors. (**A**) Top 10 GO pathways with highest normalized enrichment score (NES) and (**B**) Top selected KEGG pathways shown as multiple comparisons between enrichment scores. Graphs represent 1 experiment, n=3-4 mice/group.

GO, gene ontology.

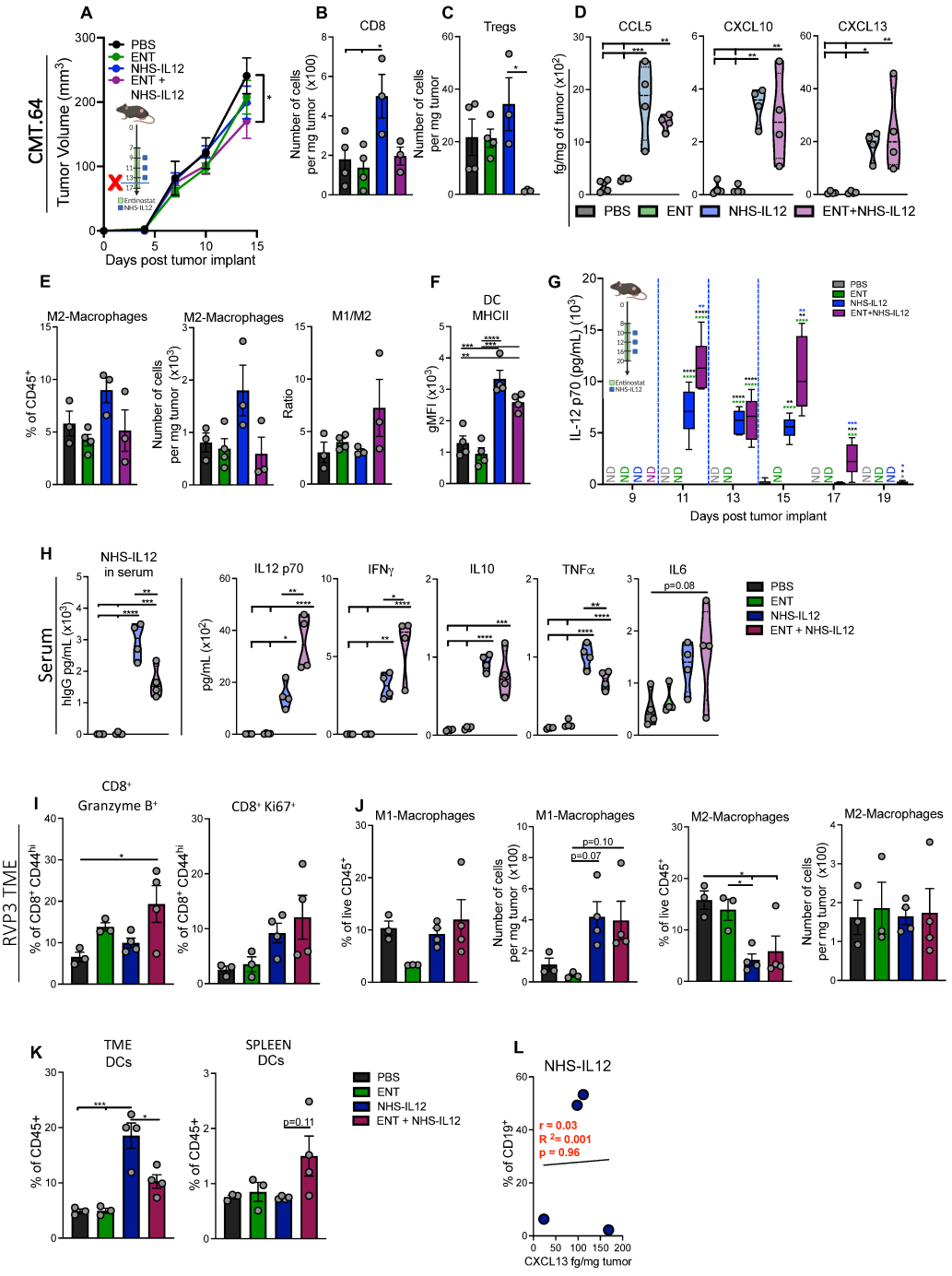

Supplemental Figure 6. Combination therapy elicited significant tumor control in the MHC-I deficient CMT.64 lung tumor model and moderate control of IFNγ-resistant RVP3

tumors. (**A** to **F, H**) CMT.64 tumor-bearing mice were treated as shown and sacrificed 2 days post last NHS-IL12 administration (day 15, *n* = 3-4 mice/group). **(A)** Treatment schedule and tumor growth curves for CMT.64-tumor bearing mice treated with PBS, entinostat (6mg/kg/day, p.o.) and/or NHS-IL12 (2 μg, s.c.). Green area represents time course of entinostat treatment while blue squares denote NHS-IL12 administration. **(B)** $CD8^+$ T cells per mg of tumor. **(C)** Tregs per mg of tumor. **(D)** Levels of designated chemokines in the TME. **(E)** M2-like macrophages as frequency of $CD45^+$ cells, cells per mg of tumor, and M1-to M2-like tumor-associated macrophages (TAMs) in the TME. **(F**) MHC-II expression (gMFI) on tumor-infiltrating DCs. **(G)** Serum IL12p70 kinetics in CMT.64 tumor-bearing mice as treated in schematic (blue dashed line indicates timing of NHS-IL12 dosing), *n* = 6 mice/group. **(H)** Serum levels of NHS-IL12 and designated cytokines. (**I-L**) RVP3 tumor-bearing mice were treated as in Fig. 6A and sacrificed 2 days post last NHS-IL12 administration (day 17), *n* = 3-4 mice/group. TME cells were analyzed by flow cytometry. (**I**) Expression frequencies of Granzyme B^+ and $Ki67^+$ in $CD8^+CD44^{hi}$ TILs. **(J)** M1- and M2-like TAM as frequency of $CD45^+$ cells and cells per mg of tumor in the TME. (**K**) DCs as frequency of $CD45^+$ cells from tumor or spleens. **(L)** Pearson correlation of CXCL13 levels to frequency of B cells ($CD19^+$) in the TME from NHS-IL12 monotherapy-treated mice. Graphs show mean ± SEM from 1 experiment; *n* = 3-4 mice/group. Tumor volume graphs: two-way ANOVA; Bar graphs and violin plots: One-way ANOVA with Tukey's multiple comparisons test; $*P < 0.05$, $**P < 0.01$, $***P < 0.001$, $****P < 0.0001$.

DCs, dendritic cells; TME, tumor microenvironment; Tregs, regulatory T cells.

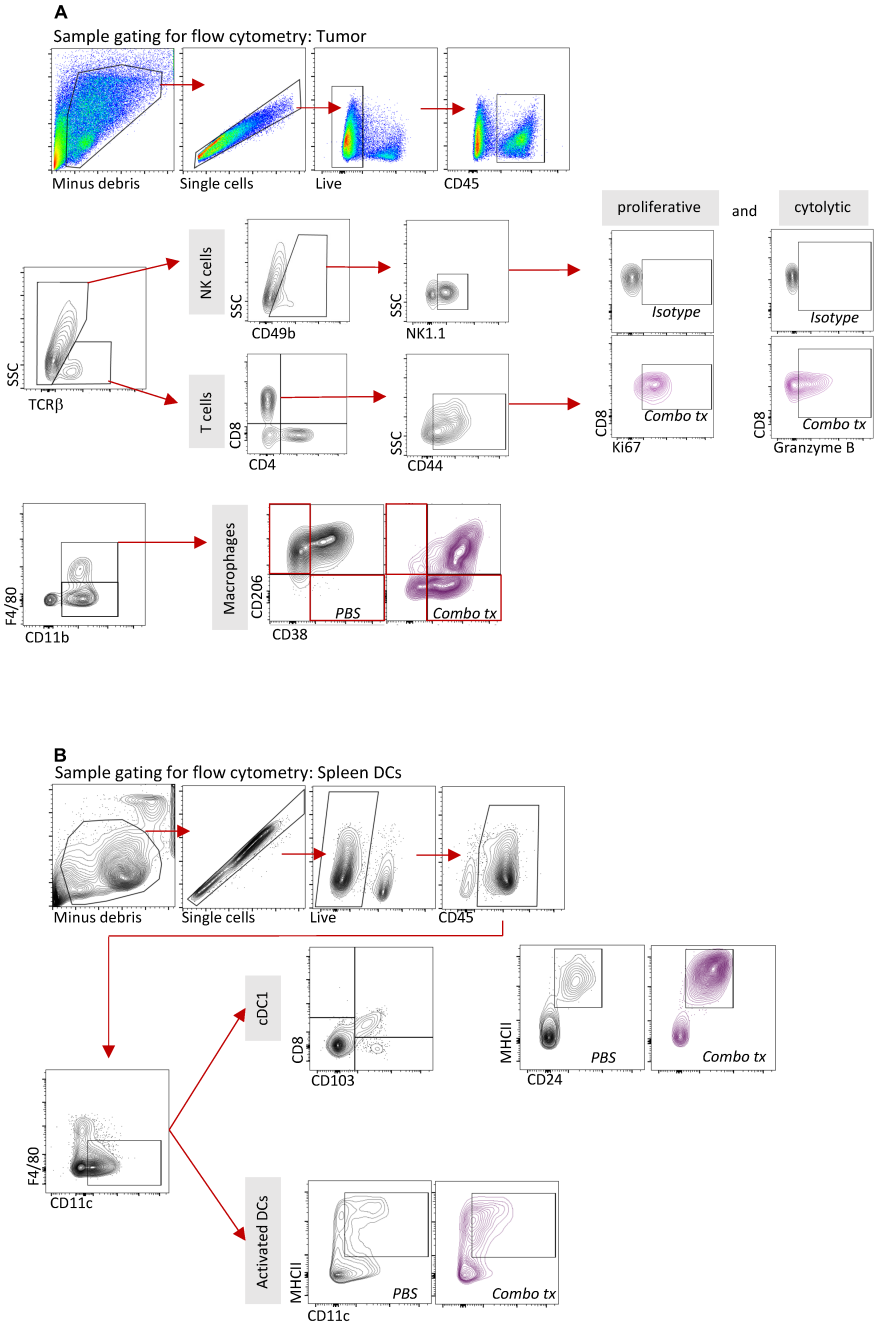

Supplemental Figure 7. Gating strategy for flow cytometry. Tumor **(A)** and spleen **(B)** gating strategy for immune subsets by flow cytometry.

Supplemental Table 1. Antibodies used for flow cytometry.

Antibody target	Clone
CD4	RM4-5
CD8a	53-6.7
CD11b	M1/70
CD11c	N418
CD19	1D3
CD24	M1/69
CD38	90
CD44	IM7
CD45.2 (Ly5.2)	104
CD49b	DX5
CD103	2E7
CD206	MR6F3
F4/80	BM8
Foxp3	FJK-16s
Granzyme B	GB11
H-2K^{b}	AF6-88.5
H-2D^{b}	KH95
IA-IE	M5/114
Ki67	SolA15
PDL1	MIH5
TCRb	IM7

Supplemental Table 2. Gating strategy for tumor and immune subtypes.

Cell type	Gating strategy
Tumor	Single cells/live/CD45^{neg}
CD4+ T	Single cells/live/CD45^{+}/TCRb^{+}/CD8^{neg}/CD4^{+}
CD8+ T	Single cells/live/CD45^{+}/TCRb$^{+/}$CD4^{neg}/CD8^{+}
Treg	Single cells/live/CD45^{+}/TCRb^{+}/CD8^{neg}/CD4^{+}/Foxp3^{+}
NK cells	Single cells/live/CD45^{+}/TCRb^{neg}/CD49b^{+}/NK1.1^{+}
M1-like macrophage	Single cells/live/CD45^{+}/CD11b^{+}/F4/80^{+}/CD38^{+}/CD206^{neg}
M2-like macrophage	Single cells/live/CD45^{+}/CD11b^{+}/F4/80^{+}/CD38^{neg}/CD206^{+}
B cells	Single cells/live/CD45^{+}/TCRb^{neg}/CD19^{+}
DCs	Single cells/live/CD45^{+}/F4/80^{neg}/CD11c^{+}/MHCII^{+}
cDC1	Single cells/live/CD45^{+}/F4/80^{neg}/CD11c^{+}/CD8^{+}/CD103^{+}/MHCII^{+}/CD24^{+}
cDC2	Single cells/live/CD45^{+}/F4/80^{neg}/CD11c^{+}/CD8^{neg}/MHCII^{+}/CD11b^{hi}

Supplemental Methods

In vitro studies. TC-1, TC-1/a9, CMT.64 and RVP3 cell lines were exposed to entinostat (500nM) or DMSO control for 48 hours prior to exposure to interferon gamma (IFNγ) (100ng/ml) or media for an additional 24 hours. At the end of treatment, cells were analyzed by flow cytometry or frozen at -80ºC in RNA*later* (Invitrogen) for subsequent RT-qPCR analysis.

Depletion studies. CD8 or CD4 depleting antibodies (100µg/100µl, i.p.) were administered on days 10, 11 and 12, followed by once weekly. For NK depletions, anti-asialo GM1 antibody (25µl in 100µl PBS) was administered on days 10 and 12 then every 3 days for 2 weeks followed by every 5 days. Depletions in peripheral blood were confirmed by flow cytometry.

Tumor re-challenge. Approximately 60 days after tumor resolution, naïve and cured mice were implanted or re-challenged, respectively, with TC1-a9 cells ($5x10^4$). Tumors were measured twice weekly using digital calipers, and volume determined as $length^2 \times width/2$.

Whole-exome sequencing (WES) and data analysis

WES. Genomic DNA was isolated from aforementioned cell lines and tails from Balb/c and C57Bl/6 mice using the DNeasy Blood and Tissue Kit (Qiagen) per the manufacturer's protocol. Whole exome sequencing was completed from aforementioned cell lines by the sequencing facility at Frederick National Laboratory for Cancer Reseach (Leidos Biomdical Research, Inc.). Briefly, exome samples were pooled and sequenced on NovaSeq 6000 S1 run using Agilent SureSelect XT Mouse All Exon and paired-end sequencing mode. The samples have 163M to 205M pass filter reads, with Q30 above 92%. The samples were mapped and variants were called

using the Dragen Bio-IT platform [1]. Percent total mapping against reference genome mm10 is about 99% and uniquely mapped reads are above 51%. Library complexity (i.e., percentage of non-duplicate reads) was determined by measuring the percentage of unique fragments in the mapped reads using MarkDuplicate utility. Percent duplicate reads are between 18% to 47%. There are 64% to 70% of reads mapped on target. Coverage statistics were also measured using Dragen. Raw sequencing depth coverage over the target region was between 501x and 628x and mapped sequencing depth coverage over target (after alignment and marking duplicates) was between 267x to 327x. The mean insert size for these samples was between 204 and 255 bases. More than 99% of the target region have the coverage above 20x. Dragen was run for all cases vs normal using the mode of somatic variant calling.

Somatic Variant Analysis. Somatic variant calling was performed using the Dragen Bio-IT platform in paired mode. Variant calls were annotated and converted to a tabular format using the *vcf2maf* tool provided by Memorial Sloan Kettering Cancer Center (github.com/mskcc/vcf2maf). The tabular data were then filtered and visualized using the 'maftools' package (version 2.8.05) and custom scripts using the R software (version 4.1.0) [2]. Specifically, variants were filtered for the following criteria: (a) depth in tumor cells >= 50; (b) variant allele frequency (VAF) in tumor cells >= 0.05; (c) variant allele depth in tumor cells >= 10; and (d) variant allele depth in normal <= 2. Burden plots and oncoplots were visualized using the R packages 'ggplot2' and 'ComplexHeatmap', respectively [3].

Real-time quantitative polymerase chain reaction (real-time qPCR). RNA was converted to cDNA using the high-capacity cDNA-to-RNA kit (Thermo Fisher Scientific) per the

manufacturer's protocol. TaqMan Gene Expression Assay (ThermoFisher Scientific) was utilized for *Psmb9* (Lmp2; Mm00479004_m1), *B2m* (Mm00437762_m1) and *Nlrc5* (Mm01243039_m1) genes for qPCR. Housekeeping genes, Gapdh (Mm99999915_g1) and *b-actin* (Mm01205647_g1) were used for determining relative fold expression using the $2^{-\Delta\Delta Ct}$ calculation method. Reactions were carried out in triplicates for genes of interest and in duplicates for housekeeping genes.

Western blots. Cell pellets were treated with RIPA buffer (Thermo Fisher Scientific) supplemented with Halt protease and phosphatase inhibitor cocktail (Thermo Fisher Scientific) according to the manufacturer's protocol. Briefly, cells were vortexed then kept on ice for 10 mins before centrifugation at ~14,000g for 15 mins. Protein was quantified using the Pierce BCA Protein Assay Kit (Thermo Fisher Scientific). Up to 50 mg of protein was loaded onto Bolt 4-12% Bis-Tris 10-well gels in MES SDS Running Buffer (Thermo Fisher Scientific). Sample gels were transferred onto nitrocellulose transfer membranes using the iBlot 2 Gel Transfer Device (Thermo Fisher Scientific) per the manufacturer's protocol. Membranes were blocked for 1 hour with BSA or milk at room temperature and probed with anti-LMP2 primary antibody (Abcam; ab242061, 1:500) overnight at 4°C. Finally, membranes were incubated with secondary antibody (LI-COR; IRDye goat anti-Rabbit IgG; 1:5000) for 1 hour at room temperature and subsequently imaged on an Odyssey Digital Imaging System (LI-COR).

Tissue processing. Single-cell suspensions from tumor and spleen tissues were prepared using standard procedures as previously described [4]. Briefly, tumors were minced in PBS with surgical scissors and subsequently homogenized using a gentleMACS Dissociator (Miltenyi Biotech).

Tumor supernatants were collected, and tumors were further digested in 2mg/mL collagenase IV and DNase at 37°C for 20-30 mins and filtered prior to staining for flow cytometry.

Flow cytometry. Cells ($1\text{-}2\times10^6$) were stained with LIVE/DEAD viability dye (ThermoFisher) per the manufacturer's instructions and subsequently incubated with Fc-block CD16/CD32 (Biolegend) for 10 mins at 4°C. Cell surface staining was performed for 30 mins at 4°C with designated antibodies (Supplementary Table 1). Intracellular staining was executed using BD cytofix/cytoperm kit per the manufacturer's instructions. The LSR Fortessa (BD Biosciences) was utilized for acquisition of 2.5×10^5 cells for spleens and $8\text{-}20\times10^4$ cells for tumors. Data were analyzed in FlowJo Analysis Software v. 10.7 (BD Biosciences) using gating strategies shown in Supplementary Table 2 and Supplementary Fig. 6.

Immunofluorescent detection of infiltrating $CD8^+$ T cells and Granzyme B. Tumor sections were fixed in Z-fix (Anatech). Tumor embedding and subsequent sectioned slides were prepared by American HistoLabs. Staining was performed on paraffin-embedded tumor tissue sections. Briefly, tissues were deparaffinized and rehydrated through a gradient of ethanol, microwaved in Rodent Decloaker antigen retrieval solution (BioCare Medical), cooled, rinsed with tris-buffered saline containing 0.1% Tween (TBST), and blocked with BLOXALL Blocking Solution (Vector Laboratories). For fluorescence detection, the Opal 4-Color Manual IHC Kit (PerkinElmer) was utilized. Staining with primary and secondary antibodies was conducted by following the manufacturers' instructions. Primary antibodies included anti-CD8a (4SM16, Invitrogen) and anti-Gzmb (16G6, eBioscience), which were used at 1:100 and 1:200 dilution, respectively, for 1 hour at room temperature. All slides were stained with DAPI (Invitrogen) and mounted in

ProLong Diamond Antifade Mountant (ThermoFisher). Slide scanning and quantification were performed on an Axio Scan.Z1 and Zen Blue v3.1 software (Zeiss). For image quantification, 5-6 equal sized regions of interest (ROI) were randomly selected per tumor in areas with no obvious signs of necrosis. Zen software was utilized to calculate the counts of $CD8^+$ cells per ROI and the mean channel fluorescence of GranzymeB expression per $CD8^+$ cell.

Cytokines and chemokines assays. Serum cytokines were quantified via Mouse V-PLEX 10-plex Proinflammatory Panel I Kit and MESO QuickPlex SQ 120 (Meso Scale Diagnostics, LLC). Limits of detection were: IFNγ: 0.04 pg/ml, IL-6: 0.61 pg/ml, IL-10: 0.95 pg/ml, TNFα: 0.13 pg/ml. Chemokines were quantified via multiplexed bead-based assays (Legendplex; Biolegend) with data acquired on a FACSVerse Flow Cytometer (BD Biosciences) per the manufacturer's instructions. Data analysis was performed using FlowJo Analysis Software v. 10.7 (BD Biosciences).

RNA isolation. Tumors were homogenized using the Tissue Ruptor II (Qiagen) system with disposable probes. Cell and tumor RNA isolated with RNeasy kit (Qiagen) in conjunction with RNase-free DNase digestion kit (Qiagen) per the manufacturer's instructions were stored at -80ºC for downstream assays. RNA was quantified using the Nanodrop Spectrophotometer (Thermo Fisher Scientific). For RNAseq experiments, RNA purity and quality were assessed on a Tapestation system (Agilent).

RNA sequencing and analysis

RNA sequencing. Tumor bulk RNA was sequenced by Novogene UC Davis Sequencing Center (Novogene Corporation, Ltd). Briefly, RNA samples were assessed for integrity and quantified using the Nano 6000 Assay Kit for the Bioanalyzer 2100 system (Agilent Technologies). The NEBNext Ultra RNA Library Prep Kit for Illumina was utilized for generating sequencing libraries. First and second strand cDNA synthesis were performed, and adaptors ligated to the adenylated 3' ends of DNA. Standardization of fragment sizes was carried out by selecting fragments of 150-200 bp for PCR. PCR was performed and final library quality was assessed utilizing the Agilent Bioanalyzer 2100 system. Clustering was carried out utilizing the cBot Cluster Generation System using PE Cluster Kit cBot-HS (Illumina) according to the manufacturer's instructions. Library preparations were sequenced, and paired-end reads were generated on an Illumina platform.

RNAseq analysis. Bioinformatics analysis and visualization were performed in the NIH Integrated Analysis Portal (NIDAP) using R programs developed on the Foundry platform (Palantir Technologies, Inc). Low count genes were filtered out across all samples and expression data was subsequently normalized using the quantile method to assess sample variances as additional quality control. Count data were transformed to log2-counts per million (logCPM) for subsequent analysis of differential expression of genes (DEG). Heatmaps, volcano plots and gene set enrichment analyses (GSEA) were carried out utilizing the DEG output. The molecular signatures database (MSigDB v6.2) with mouse/macaque orthologs was utilized as the source of enriched pathways within NIDAP.

ELISPOT. IFNγ-secreting splenocytes were quantified using the mouse IFNγ ELISPOT kit (BD Biosciences) according to the manufacturer's protocol. Briefly, splenocytes ($1x10^6$) were cocultured with overlapping HPV16 E7 15-mer peptide (JPT Peptide Technologies Inc.) for 24 hours [5]. Spot counts were imaged and quantified using an ImmunoSpot analyzer (Cellular Technology Limited (CTL)).

Data availability statement Human gene transcript TCGA (https://portal.gdc.cancer.gov) and GTEx (http://gtexportal.org) datasets are identified in figure legends and were accessed through TIMER2.0 (http://timer.comp-genomics.org) or GEPIA2 (http://gepia2.cancer-pku.cn). Whole-exome and RNA sequencing data are deposited at https://dataview.ncbi.nlm.nih.gov/object/PRJNA795151?reviewer=64c1r16fh3gaokotfdjtpcq7na. All additional data are available from the authors upon reasonable request.

Code availability All RNASeq data analysis and visualization were performed utilizing the NIH Integrated Data Analysis Platform (NIDAP) using R programs developed on the Foundry platform. All scripts used have been deposited on Github (https://github.com/NIDAP-Community/Entinostat-and-NHS-IL12-in-aPD1-aPDL1-refractory-models).

Supplemental References

1. Miller, N.A., Farrow, E.G., Gibson, M., Willig, L.K., Twist, G., Yoo, B., *et al.* A 26-hour system of highly sensitive whole genome sequencing for emergency management of genetic diseases. *Genome Med* **7**, 100 (2015).

2. Mayakonda, A., Lin, D.C., Assenov, Y., Plass, C., and Koeffler, H.P. Maftools: efficient and comprehensive analysis of somatic variants in cancer. *Genome Res* **28**, 1747-1756 (2018).

3. Gu, Z., Eils, R., and Schlesner, M. Complex heatmaps reveal patterns and correlations in multidimensional genomic data. *Bioinformatics* **32**, 2847-2849 (2016).

4. Knudson, K.M., Hicks, K.C., Luo, X., Chen, J.Q., Schlom, J., and Gameiro SR. M7824, a novel bifunctional anti-PD-L1/TGFbeta Trap fusion protein, promotes anti-tumor efficacy as monotherapy and in combination with vaccine. *Oncoimmunology* **7**, e1426519 (2018).

5. Smalley Rumfield, C., Pellom, S.T., Morillon II, Y.M., Schlom, J., and Jochems, C. Immunomodulation to enhance the efficacy of an HPV therapeutic vaccine. *J Immunother Cancer* **8** (2020).